Published online 29 July 2017

Nucleic Acids Research, 2017, Vol. 45, No. 16 ***9467–9480***
doi: 10.1093/nar/gkx660

Systematic analysis of DNA crosslink repair pathways during development and aging in *Caenorhabditis elegans*

David M. Wilson, III[1,*,†], Matthias Rieckher[2,†], Ashley B. Williams[2] and Björn Schumacher[2,*]

[1]Laboratory of Molecular Gerontology, National Institute on Aging, Intramural Research Program, National Institutes of Health, Baltimore, MD 21224, USA and [2]Institute for Genome Stability in Aging and Disease, Medical Faculty, Cologne Excellence Cluster for Cellular Stress Responses in Aging-Associated Diseases (CECAD), Center for Molecular Medicine Cologne (CMMC) and Systems Biology of Ageing Cologne (Sybacol), University of Cologne, Joseph-Stelzmann-Strasse 26, 50931 Cologne, Germany

Received March 22, 2017; Revised July 16, 2017; Editorial Decision July 17, 2017; Accepted July 18, 2017

ABSTRACT

DNA interstrand crosslinks (ICLs) are generated by endogenous sources and chemotherapeutics, and pose a threat to genome stability and cell survival. Using *Caenorhabditis elegans* mutants, we identify DNA repair factors that protect against the genotoxicity of ICLs generated by trioxsalen/ultraviolet A (TMP/UVA) during development and aging. Mutations in nucleotide excision repair (NER) components (e.g. XPA-1 and XPF-1) imparted extreme sensitivity to TMP/UVA relative to wild-type animals, manifested as developmental arrest, defects in adult tissue morphology and functionality, and shortened lifespan. Compensatory roles for global-genome (XPC-1) and transcription-coupled (CSB-1) NER in ICL sensing were exposed. The analysis also revealed contributions of homologous recombination (BRC-1/BRCA1), the MUS-81, EXO-1, SLX-1 and FAN-1 nucleases, and the DOG-1 (FANCJ) helicase in ICL resolution, influenced by the replicative-status of the cell/tissue. No obvious or critical role in ICL repair was seen for non-homologous end-joining (*cku-80*) or base excision repair (*nth-1*, *exo-3*), the Fanconi-related proteins BRC-2 (BRCA2/FANCD1) and FCD-2 (FANCD2), the WRN-1 or HIM-6 (BLM) helicases, or the GEN-1 or MRT-1 (SNM1) nucleases. Our efforts uncover replication-dependent and -independent ICL repair networks, and establish nematodes as a model for investigating the repair and consequences of DNA crosslinks in metazoan development and in adult post-mitotic and proliferative germ cells.

INTRODUCTION

Damage to genetic material can arise from spontaneous hydrolysis or through reactions with chemical or physical agents produced intracellularly or found within the environment (1,2). Such damage includes a range of simple and bulky (helix-distorting) base modifications, abasic sites, phosphodiester strand breaks and interstrand crosslinks (ICLs), to name a few. Persistent DNA modifications can lead to mutagenic changes in the cell's genetic blueprint or cause arrest of the transcriptional or replicative machinery, which can activate cell death responses. These outcomes underlie disease development and likely contribute to the aging process (3).

ICLs covalently link the two-paired strands of DNA (4). As such, they pose a major impediment to transcription and replication, which require strand separation to be efficiently executed. Since ICLs are likely formed naturally in cells through reactions with endogenous chemicals, such as the lipid peroxidation product malondialdehyde (5), or via reactions of the aldehyde group of a spontaneously-formed or enzyme-derived abasic site in DNA with a normal base on the opposite strand (6,7), organisms have evolved elaborate mechanisms to remove these deleterious lesions from the genome. The most well characterized pathways are those linked to DNA replication, called into play when the replication fork collides with an ICL (8,9). In situations of dual-fork (and most likely single-fork) convergence, the stalled replicative CMG (MCM2–7) helicase is displaced by a BRCA1/BARD1 complex, facilitating the eventual activation of the Fanconi anemia (FA) pathway. FA is a genetic disorder characterized by congenital ab-

*To whom correspondence should be addressed. Tel: +1 410 558 8153; Fax: +1 410 558 8157; Email: wilsonda@grc.nia.nih.gov
Correspondence may also be addressed to Björn Schumacher. Tel: +49 221 478 84202; Fax: +49 221 478 84204; Email: bjoern.schumacher@uni-koeln.de
†These authors contributed equally to the paper as first authors.

normalities, bone marrow failure, cancer predisposition and profound sensitivity to crosslinking agents (10–13). Following assembly of the repair machinery at the site of the ICL, the crosslink is unhooked by incisions on the strand opposite the approached replication fork via nucleases that remain controversial, yet likely include the multi-functional ERCC1/XPF complex (14–16), leading to the formation of a DNA double-strand break. The current model, which is largely based on genetic studies, proposes that bypass synthesis is then carried out across the crosslink remnant by a translesion DNA polymerase to generate an intact duplex that is used as a template for resolving the double-strand break via RAD51-mediated homologous recombination (HR), prior to the resumption of DNA synthesis (17). Global genome nucleotide excision repair (GG-NER) is presumed to remove the lingering remnant (4). Notably, recent evidence indicates that in most situations when a replication fork encounters an ICL, FANCM facilitates replicative traverse via an unknown mechanism, leading to the formation of a DNA intermediate that ultimately requires the same processing steps as outlined above (18).

In addition to the replication-associated responses, replication-independent mechanisms exist that involve ICL identification by either GG-NER recognition proteins or a transcription-coupled NER (TC-NER) process that is called into action upon RNA polymerase arrest at the site of the blocking lesion. In the former situation, the GG-NER recognition complex comprised of XPC and RAD23 initiates a classic NER response that involves incision events executed by ERCC1/XPF and potentially XPG to mediate unhooking (19). Alternatively, the 5′-3′ exonuclease SNM1A, a PSO2 homolog, follows 5′ incision by the ERCC1/XPF complex to guide unhooking by nuclease degradation through the ICL (20). In either case, once unhooked, the generated DNA gap is filled by a translesion DNA polymerase, which carries out synthesis across the crosslink remnant, prior to sealing of the nick and a subsequent round of GG-NER. In situations where RNA polymerase II encounters the ICL, transcription likely arrests, activating a transcription-associated response that aims to resolve the lesion prior to the resumption of RNA synthesis (21). In the classic TC-NER response, factors central to facilitating the repair process are CSA and CSB, proteins defective in the premature aging disorder Cockayne syndrome (CS). Following the initial recognition event, the steps of ICL removal in the transcription-associated response would presumably be similar to that of GG-NER, i.e. incision, unhooking, gap-filling, ligation and another round of classic GG-NER. While evidence indicates that mismatch repair (MMR) recognition complexes, such as MSH2/MSH3 (a.k.a. MutSβ), can specifically bind to DNA ICLs (22–24), the role of the pathway in either facilitating removal of these lesions or activating cell death responses remains unclear (25–29).

Psoralen is the parent compound in a family of natural products known as furanocoumarins (depicted in Figure 1A) (30). It is produced naturally in the seeds of the plant, *Psoralea corylifolia* and is found in celery, parsley and all citrus fruits. Psoralen is a photoactivatable agent, which when combined with UV light, can be used to treat several hyperproliferative skin conditions, including psoriasis, eczema and vitiligo, as well as cutaneous T-cell lymphoma. Evidence indicates that the clinical efficacy of psoralen is related to its ability to intercalate into DNA and, upon activation by UVA irradiation, generate lethal monoadducts and ICLs. Trioxsalen, 4, 5′, 8-trimethylpsoralen (TMP), is a psoralen derivative (Figure 1B). Its unique chemistry permits a very high degree of ICL formation relative to DNA monoadducts (estimated to be 10:1 in human cells) upon UVA activation (18). Other DNA crosslinking agents, such as cisplatin and mitomycin C, produce only a small fraction of ICLs among the total number of DNA adducts formed, in addition to inducing conditions of oxidative stress (4). Considering the intrinsic characteristics of the various crosslinking agents, TMP is a powerful tool to examine mechanisms specifically related to ICL repair, with a limited concern for the ancillary issues related to monoadduct formation.

While much work has gone into characterizing the repair mechanisms for ICLs, there remain questions and controversies regarding the players that are involved in ICL recognition and resolution. We have employed the nematode, *Caenorhabditis elegans*, as a genetically-tractable, multicellular model organism to determine the contribution of specific DNA repair factors in the resistance to the crosslinking agent TMP + UVA (TMP/UVA). Prior work in *C. elegans*, which retain many of the basic DNA damage response mechanisms (31,32), has revealed contributions of the MRT-1 (SNM1 homolog) and FAN-1 nucleases (33,34), as well as a number of conserved FA gene homologs, such as FCD-2 (FANCD2), the DOG-1 helicase (FANCJ/BRIP1/BACH1) and FNCM-1 (FANCM) (35–37), in ICL repair. However, a broader, comparative assessment of factors and associated repair pathways that may contribute to the removal of toxic ICLs has not been explored in worms.

C. elegans shares many of the essential biological processes that are central to human biology, including embryogenesis, morphogenesis, development, nerve function, behavior and aging. Moreover, the nematode allows the analysis of the consequences of DNA damage in distinct tissue types during animal development and aging (see Supplementary Figure S1 for life cycle). In particular, most somatic cell divisions occur during early embryonic development, while during larval development, differentiated cells mostly grow in size. In adult worms, somatic tissues are terminally-differentiated, whereas germ cells continue to undergo mitotic and meiotic cell divisions. *C. elegans* therefore provides a powerful model for interrogating the roles of DNA repair systems in proliferated germ cells, during meiotic recombination and in the maintenance of differentiated cell types. Following the establishment of an effective treatment regimen, we screened a series of DNA repair mutant strains for sensitivity to TMP/UVA relative to treatment with the vehicle plus UVA only (DMSO/UVA). Our studies provide new insight into the genetic factors and associated molecular pathways needed for protection against the devastating biological consequences of DNA ICLs.

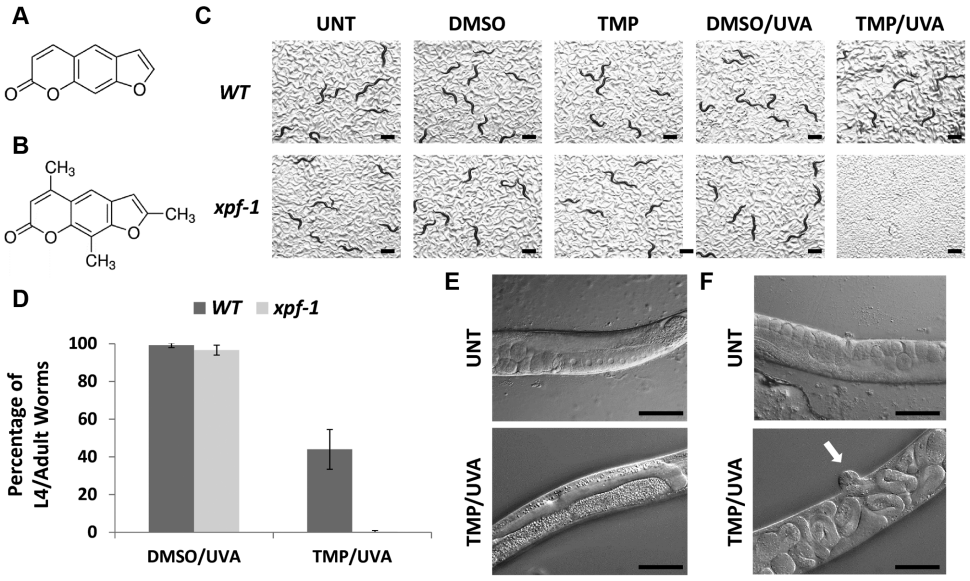

Figure 1. Effect of the different treatment paradigms on wild-type (WT) and *xpf-1* mutant worms. Chemical structures of psoralen (**A**) and TMP (**B**). (**C**) Visual images. Scenarios include untreated control, DMSO only (no UVA), TMP only (no UVA), DMSO plus UVA (DMSO/UVA) and TMP/UVA. Photographs were taken at day 3 after the designated treatment paradigm (see Supplementary Figure S2 for representative experiment). Black bar = 1 mm. (**D**) Sensitivity plots. Shown are the averages and standard deviations from either five (*xpf-1*) or eight (WT) independent experimental data points. The images and results depicted (percentage of L4/adult worms of total) were obtained after exposure of L1 worms to DMSO or TMP (30 μg/ml) for 60 min, and then UVA irradiated for 60 s (as indicated). *P*-value (TMP/UVA) = 0.00008. Pathophysiological consequences of TMP/UVA exposure on the germline (**E**) and vulva (**F**) of WT worms. Differential interference contrast (DIC) images are shown of untreated (UNT), age-matched WT worms or WT L1 worms that were subjected to the standard protocol of TMP/UVA (see above) and then photographed 3 days after treatment. In the UNT animals, note the normal germline, oocyte and embryo organization (panel E) and the normal vulva and internal structure (panel F). The white arrow designates the protruding vulva of the TMP/UVA treated worm. Black bar = 100 micron.

MATERIALS AND METHODS

Nematode strains and reagents

C. elegans were maintained according to standard protocols (38). The strains and associated mutant alleles were as follows (see also Table 1): N2: wild-type (WT) Bristol isolate, *brc-1(tm1145) III., brc-2(tm1068)* III/hT2 *[bli-4(e937) let-?(q782) qls48] (I;III), cku-80(ok861), csa-1(tm5232) II., csb-1(ok2335) X., dog-1(gk10) I., ercc-1(tm2073) I., ercc-1(tm1981) I., exo-1(tm1842) III., exo-3(ok3539) I., fan-1(tm423) IV., fcd-2(tm1298) IV., gen-1(tm2940) III., him-6(e1104) IV., him-18(tm2181)*/qC1 *[dp7–19(e1259) glp-1(q339)* qls26] *III., mrt-1(e1354) I.,msh-2(ok2486) I., mus-81(tm1937) I., nth-1(ok724) III., slx-1(tm2644) I., wrn-1(gk99) II., xpa-1(ok698) I., xpc-1(tm3886) IV., xpf-1(tm2842) II., xpf-1(e1487) II., xpg-1(tm1670) I.* The Bristol N2 isolate is the standard WT reference strain used in the community, and all mutant strains employed have been derived from this isolate. Mutant alleles have been generated via previous mutagenesis screens relying on monofunctional alkylating agent treatment (e.g. ethylmethanesulfonate), and deletion alleles have been produced by various consortia typically using TMP/UV mutagenesis. The mutant alleles have been backcrossed several times, and all mutant strains are publicly available from the *C. elegans* Genome Center (Wisconsin) or the National Biosource (Japan), and more completely described at wormbase.org. TMP (cat. no. T6137) was purchased from Sigma.

Treatment protocol

Animals were synchronized at L1 stage via standard hypochlorite treatment (39). Stock TMP was prepared the day of use in dimethyl sulfoxide (DMSO) at a final concentration of 2 mg/ml. Approximately 500–1000 L1 worms were incubated in a final volume of 400 μl with freshly prepared TMP at a final concentration of 30 μg/ml for 1 h while rotating. After transfer to a 6-well plate, worms were exposed to UVA (365 nm) for 60 s (∼480 J/m^2; unless indicated otherwise). Worms were collected and washed with M9 medium, before being plated on NGM-OP50 plates to monitor and record development and viability with a stereomicroscope. Worms were maintained at 20°C in the dark and monitored as needed. To study the DW104 (*brc-2* mutant) and CV98 (*him-18* mutant) strains, we treated ∼2000 animals with TMP/UVA as above, and recorded development and viability via fluorescent stereomicroscopy to distinguish the balanced heterozygous (GFP-positive) from the homozygous mutant populations (GFP-negative). In the case of synchronized young adults, ∼200 worms were treated as above with TMP/UVA, with UVA exposure being carried out for 4 min. Statistical comparisons, where appropriate, were conducted in Excel using the *t*-test: Two-Sample Assuming Unequal Variances program.

Visualization of genotoxic agent effects

Worms were mounted on 2% agarose pads and imaged using a Zeiss Axio Imager Z.2 equipped with differential interference contrast (DIC) optics in 10× and 40× objectives.

Table 1. Mutant strain summary

Gene name (human equivalent)	Biochemical function	Primary pathway(s)	Strain	Allele	TMP/UVA sensitivity (L1 treatment)
xpa-1	Damage recognition	NER	RB864	*ok698*	Severe (L2)
xpc-1	Damage recognition	NER	FX03886	*tm3886*	High
csa-1	Ubiquitin ligase complex	TC-NER	FX0532	*tm5232*	None
csb-1	SWI1/SNF2 ATPase	TC-NER	RB1801	*ok2335*	None
xpf-1	Endonuclease	NER; ICLR	TG1660, CB1487	*tm2842, e1487*	Severe (L1/L2)
ercc-1	XPF-1 partner	NER; ICLR	FX02073, TG163	*tm2073, tm1981*	Severe (L2/L3)
xpg-1	RAD2 endonuclease	NER	TG1565	*tm1670*	Severe (L1/L2)
nth-1	Glycosylase	BER	RB877	*ok724*	None
exo-3 (*APE1*)	AP endonuclease, exonuclease	BER	RB2548	*ok3539*	None
msh-2	Mismatch recognition	MMR	RB1913	*ok2486*	None to moderate
cku-80	DSB end-binding factor	NHEJ	RB964	*ok861*	None
brc-1 (*BRCA1*)	Scaffold	HR	DW102	*tm1145*	Moderate
brc-2 (*BRCA2/FANCD1*)	Scaffold	HR; ICLR	DW104	*tm1086*	None
fcd-2 (*FANCD2*)	Effector factor	ICLR	NB105	*tm1298*	None to moderate
dog-1 (*FANCJ*)	Helicase	ICLR	VC13	*gk10*	High
him-6 (*BLM*)	Helicase	Replication fork	CB1138	*e1104*	None
wrn-1	Helicase	Replication fork	VC174	*gk99*	None
exo-1	Nuclease	MMR; HR	SSM72	*tm1842*	Moderate
fan-1	Nuclease	ICLR	TG1568	*tm423*	Germline-specific
gen-1	Nuclease	HR	TG1540	*tm2940*	None
mrt-1 (SNM1)	Nuclease	ICLR	YA1116	*tm1354*	None
mus-81	Nuclease	ICLR	TG1760	*tm1937*	High
slx-1	Nuclease	ICLR	TG1868	*tm2644*	Germline-specific
him-18 (*SLX4*)	SLX-1 partner	ICLR	CV98	*tm2181*	None

Information regarding gene name in *C. elegans*, the human gene equivalent (where significantly different), the primary DNA repair pathway associated with the encoded protein (in humans), and the worm strain and mutant allele (used herein) is provided. In addition, the degree of sensitivity to the standard TMP/UVA treatment relative to WT is listed, as well as the latest stage of developmental arrest where relevant. AP = apurinic/apyrimidinic; DSB = double-strand break.

Assessment of pharyngeal pumping

Animals were hypochlorite-synchronized and grown to young adult stage. Approximately 500 animals were exposed to the DMSO or TMP treatment protocol, followed by 120 s UVA exposure (~960 J/m^2). Subsequently, animals were plated and pharyngeal pumping of 15 individual worms per strain and condition was assessed 48 and 72 h post-treatment by counting grinder movements under the stereomicroscope for 30 s per animal.

Measurement of adult survival

After hypochlorite-synchronization, animals were grown to young adult stage and subjected to DMSO or TMP treatments, followed by 120 s UVA exposure (~960 J/m^2). Animals were subsequently plated on OP50-seeded plates. Next, ~150 animals per strain and condition were counted and transferred to fresh OP50-seeded plates every second day until day 8 of adulthood. From then on, animals were transferred every fourth day and continuously counted every second day until death. Dead animals were tested for touch response by poking with a platinum wire and close observation of residual pumping movements in the pharynx. Dead animals were scored and removed from the plate. We censored animals that died from internal hatching or escaped from the plate.

Measurement of embryonic lethality

Animals were hypochlorite-synchronized and grown for 72 h at 20°C into day 1 adults, and then treated with TMP/UVA at 0, 30, 60 and 120 (~960 J/m^2) s of irradiation. Animals were allowed to recover for 3 or 24 h on OP50-seeded plates. Subsequently, four animals of each treatment were transferred in triplicate to fresh OP50 seeded 60 mm plates and allowed to lay eggs for 2 h. After removal of the adults, the number of eggs was counted, and 48 h later the number of offspring was counted to quantify hatching efficiency.

RESULTS

Development of a TMP/UVA screening strategy

Psoralen has previously been used to induce mutagenesis in *C. elegans* (40). To verify that the combination of TMP and UVA irradiation would elicit a measurable response, we initially determined the relative sensitivities of Bristol N2 WT and *xpf-1(tm2842)* mutant L1 worms to TMP/UVA treatment. XPF is a binding partner of ERCC1, and the heteroprotein complex has been reported to operate as an endonuclease in processes involved in bulky adduct removal (i.e. NER) and ICL resolution (16). Moreover, studies in yeast and mammalian cells indicate a clear role for the nuclease complex in crosslinking agent resistance. To confirm a conserved function in *C. elegans* and to establish the TMP/UVA assay, we employed mutant worms that carried the deletion allele *xpf-1(tm2842)* (from here on *xpf-1*).

The treatment protocol is described in detail in the 'Materials and Methods' section. Briefly, arrested L1 larvae were prepared, incubated in M9 medium with vehicle only (DMSO) or TMP for the indicated time (typically 60 min), exposed to UVA (365 nm) irradiation as designated (typically 60 s), washed and then plated to monitor development and survival. Some general observations regarding the L1 screening strategy include: (i) TMP exposure alone, i.e. without UVA irradiation, had no obvious effect on worm viability or function; (ii) incubation of worms with TMP for 15 min was insufficient for an optimal TMP/UVA effect (likely due to poor up-take and/or distribution of the chemical agent), whereas 60 min incubations resulted in a detectable biological outcome; and (iii) at least a 20 s UVA

exposure (∼160 J/m^2) was required to activate the TMP compound and produce an observable effect.

Once the treatment strategy was established, we compared the TMP/UVA sensitivity of WT and *xpf-1* L1 worms, evaluating varying doses of UVA (365 nm) irradiation. Our experiments revealed a clear and dramatic UVA dose-dependent hypersensitivity of the mutant worms to the combination of TMP/UVA relative to the WT control animals. Indeed, after incubation with TMP (final concentration of 30 μg/ml) for 60 min, a complete absence of fully-developed L4 larval stage or adult worms was observed for the DNA repair mutant 3 days after UVA exposures of 60 s (480 J/m^2) or longer (Figure 1C and D; Supplementary Figure S2). Based on visual inspection of the *xpf-1* mutants at 3, 6 and 10 days post-TMP/UVA60 or TMP/UVA90 treatment, irreversible developmental arrest occurred around L1/L2, although precise staging is complicated by the overall poor condition of the surviving animals. In addition, no progeny (i.e. egg laying) was observed in the *xpf-1* TMP/UVA-treated samples during the 10 days of monitoring, consistent with the limited development and a dysfunctional germline. While the WT strain did experience a TMP/UVA dose-dependent sensitivity, L4 and adult worms were observed even at the 90 s UVA (∼720 J/m^2) exposure (Supplementary Figure S2; ∼22% of total in representative experiment shown), as were progeny, although severe somatic and germline defects were evident in a large portion of the survivors.

Pathophysiological consequences of TMP/UVA treatment

To gain insight into how TMP elicits its detrimental physiological effects, we visualized WT worms via DIC microscopy 3 days after the standard TMP/UVA60 treatment of L1 animals. Beyond lethality (i.e. the presence of corpses), the obvious physical anatomical abnormalities and impaired mobility, inspection of adult or near-adult worms revealed three major classes: (i) normal worms (ii) worms with a disrupted germline (Figure 1E); and (iii) bags of worms resulting from internal hatching, associated with a protruding vulva and matricide (Figure 1F, see arrow). Indeed, class (iii) worms were quite common among the TMP/UVA60-treated survivors. Analysis of the less developed, younger appearing WT worms also revealed phenotypes of internal hatching, germline disruption, empty uterus, high numbers of sperm, a dumpy physical appearance and the exploded phenotype (unpublished observations). Thus, TMP/UVA treatment causes both somatic (e.g. reduced growth and uterus muscle failure) and germline defects, which are apparently exacerbated in a relevant DNA repair-deficient background, such as *xpf-1*. The pathophysiological analysis demonstrates premature functional deterioration of multiple tissues consistent with widespread homeostatic disturbance by ICL-associated genotoxic stress.

Identification of TMP/UVA-sensitive DNA repair mutants

The observed dramatic difference in sensitivity to TMP/UVA between the WT and *xpf-1* mutant worms encouraged us to apply this approach to identify genetic factors in *C. elegans* that contribute to ICL repair. We examined a set of mutants for conserved genes that span the different DNA repair pathways (summarized in Table 1), evaluating development and survival of L1 worms after the standard treatment protocol (TMP/UVA60): a 60 min incubation with 30 μg/ml TMP and a 60 s UVA (480 J/m^2) exposure. Our studies revealed a similar high sensitivity of the *xpf-1, ercc-1(tm2073), xpg-1(tm1670)* and *xpa-1(ok698)* mutant strains (Figure 2A, P-value < 0.00005). Specifically, in these four cases, arrest occurred early in the developmental process (Table 1 and Supplementary Figure S3), and no progeny were seen up to 10 days post-treatment, indicative of severe consequences of the TMP/UVA60 exposure to both mitotic and meiotic cell lineages. A pronounced and significant sensitivity was also observed for *xpc-1(tm3886)* > *dog-1(gk10)* > *mus-81(tm1937)* (P-value ≤ 0.005), although there were a few surviving worms that developed to at least L4/adult and offspring were present by day 10 (Table 1, Figure 2A and Supplementary Figure S3). Although borderline significant in terms of developmental arrest, a clear and reproducible sensitivity was caused by the *brc-1(tm1145)* (P-value = 0.055) and *exo-1(tm1842)* (P-value = 0.018) alleles. While *fcd-2(tm1298)* (P-value = 0.97) and *msh-2(ok2486)* (P-value = 0.26) showed no statistically significant defect in terms of animal development following TMP/UVA exposure (Figure 2A), the former exhibited an increase in the frequency of exploding worms (Avid phenotype) and the latter displayed what appeared to be reduced egg laying in comparison to WT. The *slx-1(tm2644)* and *fan-1(tm423)* mutants presented a composite phenotype, with worms developing similarly to WT animals after the TMP/UVA60 treatment (P-value = 0.77 and 0.98, respectively; Figure 2A), yet showing severe, selective germline defects (see below) that resulted in sterility. Consistent with the *slx-1* findings, mutation of its binding partner *him-18(tm2181)* (homolog of human SLX4), imparted no sensitivity to TMP/UVA60 in terms of animal development; germline-specific sensitivity could not be determined due to the intrinsic embryonic lethality of the *him-18* mutant strain (41). No obvious effect in larval development or germline integrity was seen with the *csa-1(tm5232)* (P-value = 0.61), *csb-1(ok2335)* (P-value = 0.68), *nth-1(ok724)* (P-value = 0.89), *exo-3(ok3539)* (P-value = 0.067), *cku-80(ok861)* (P-value = 0.63), *brc-2(tm1086)* (P-value = 0.52), *gen-1(tm2940)* (P-value = 0.99), *mrt-1(tm1354)* (P-value = 0.72), *wrn-1(gk99)* (P-value = 0.83) and *him-6(e1104)* (P-value = 0.83) single mutants when treated with the same dose of TMP/UVA60 (Table 1, Figure 2A, Supplementary Figure S3 and unpublished observations).

Using DIC microscopy, we imaged individual adults of the strains that showed high or modest sensitivity (i.e. *dog-1*, *mus-81*, *brc-1*, *exo-1*, *msh-2*, *fan-1* and *slx-1*) 3 days post-genotoxic treatment. Some of the general observations were as follows: (i) each strain exhibited phenotypes similar to those observed in WT worms, such as disrupted germline, egg retention and protruding vulva (see previous section), with these outcomes typically more pronounced in the repair-deficient strains; (ii) *msh-2* mutant animals exhibited a near WT appearance, but showed increased propensity for a protruding vulva and possibly egg retention (con-

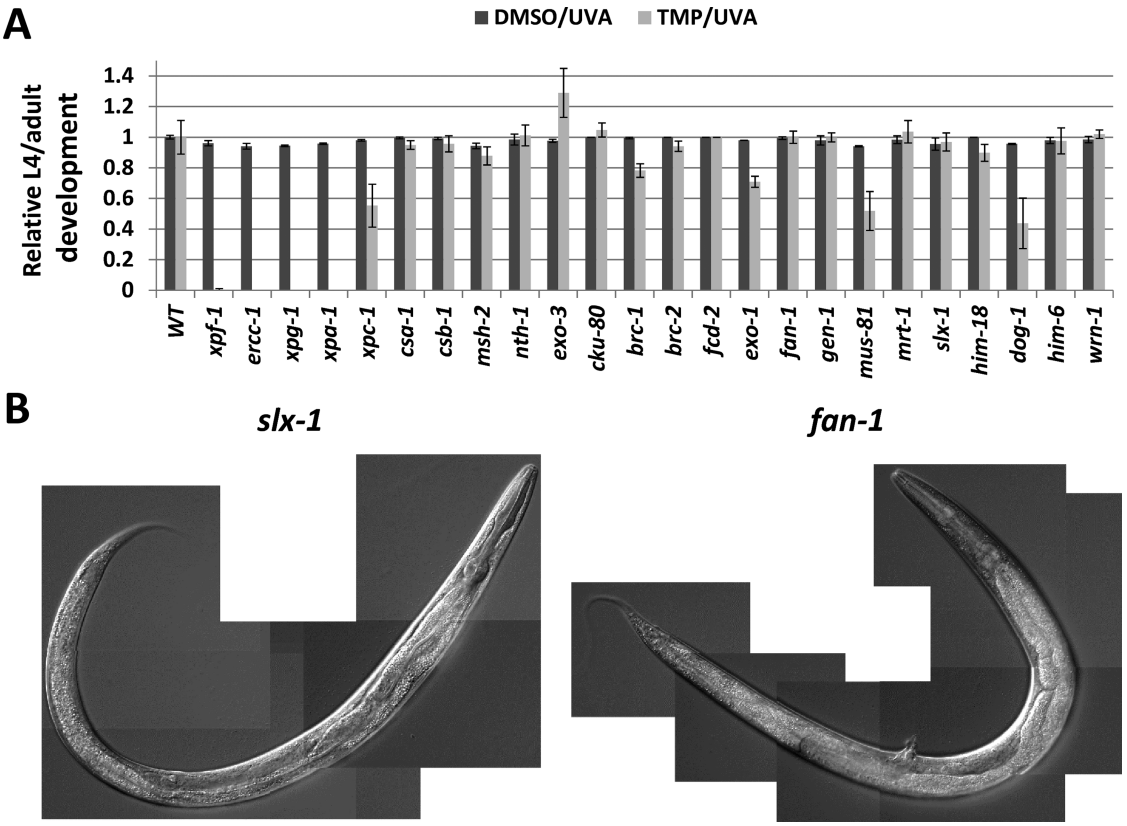

Figure 2. Response of various DNA repair-defective strains to TMP/UVA. (**A**) Relative L4/adult development. Shown are the averages and standard deviations of the relative development (mutant L4/adult percentage relative to WT) of at least three independent experimental data points. The *P*-values from the 'two-tail test' using the '*t*-test: Two-Sample Assuming Unequal Variances' program in Excel are provided in the text. (**B**) Representative DIC images of *slx-1* and *fan-1* mutant worms. Images were taken 3 days after standard TMP/UVA treatment of L1 worms.

sistent with reduced egg laying; see previous section); (iii) *dog-1* and *exo-1* mutant animals displayed increased susceptibility for rupture in comparison to WT and the other strains, suggesting a weakening of the cuticle; and (iv) *fan-1* and *slx-1* mutant animals had WT-like mitotic features, yet possessed no or a disorganized, non-functional germline (resulting in sterility), with little polarity or directionality, a phenotype that was more severe than for the other mutant strains (*fan-1* was slightly worse than *slx-1*); *fan-1* animals also displayed an increased likelihood of a protruding vulva (Figure 2B). Finally, we note that a more detailed analysis into the large number of male worms consistently present in the *xpf-1* population revealed that this strain exhibits a high-incidence-of-males (HIM) phenotype, presumably stemming from a DNA repair defect and intrinsic genome instability (41).

Roles for both GG- and TC-NER in TMP/UVA resistance

Our prior work with the human CSB protein, which operates as a key mediator of TC-NER and is defective in CS, revealed a role for the SWI2/SNF2 ATPase family member in ICL repair, particularly in non-cycling cells (42). We therefore explored further the possible contribution of CSB to TMP/UVA resistance in worms. XPC is a major recognition factor for the GG-NER response, and our screening assay revealed a significant role for this protein in protecting L1 worms from the developmental toxicity of TMP/UVA (see previous section), although to a lesser extent than other NER factors, such as XPA, which participates in both GG-NER and TC-NER (43). We did not see an obvious role for CSB in protection against the genotoxic consequences of the DNA crosslinking paradigm (see previous section), possibly implying a back-up role for TC-NER in the removal of ICLs. To examine this possibility, we determined the sensitivity of WT, *xpc-1* and *csb-1* single mutant, and *xpc-1(tm3886);csb-1(ok2335)* double mutant worms to TMP/UVA60 using our standard L1 protocol (Figure 3). These experiments uncovered a more severe sensitivity of the double mutant strain to TMP/UVA60 in comparison to the WT, *csb-1* or *xpc-1* strains, with developmental arrest occurring at or before the L2 stage (similar to the *xpa-1* strain; see previous section). Thus, our genetic data indicate that while GG-NER plays a more prominent role in ICL repair responses during animal development, the two sub-pathways of NER can play compensatory roles in ICL removal.

Effect of TMP/UVA treatment on adult pharyngeal pumping and egg laying

We next extended our analysis to young adults, which are, except for the germline, post-mitotic. We initially evaluated the effects of DNA crosslink induction on pharyn-

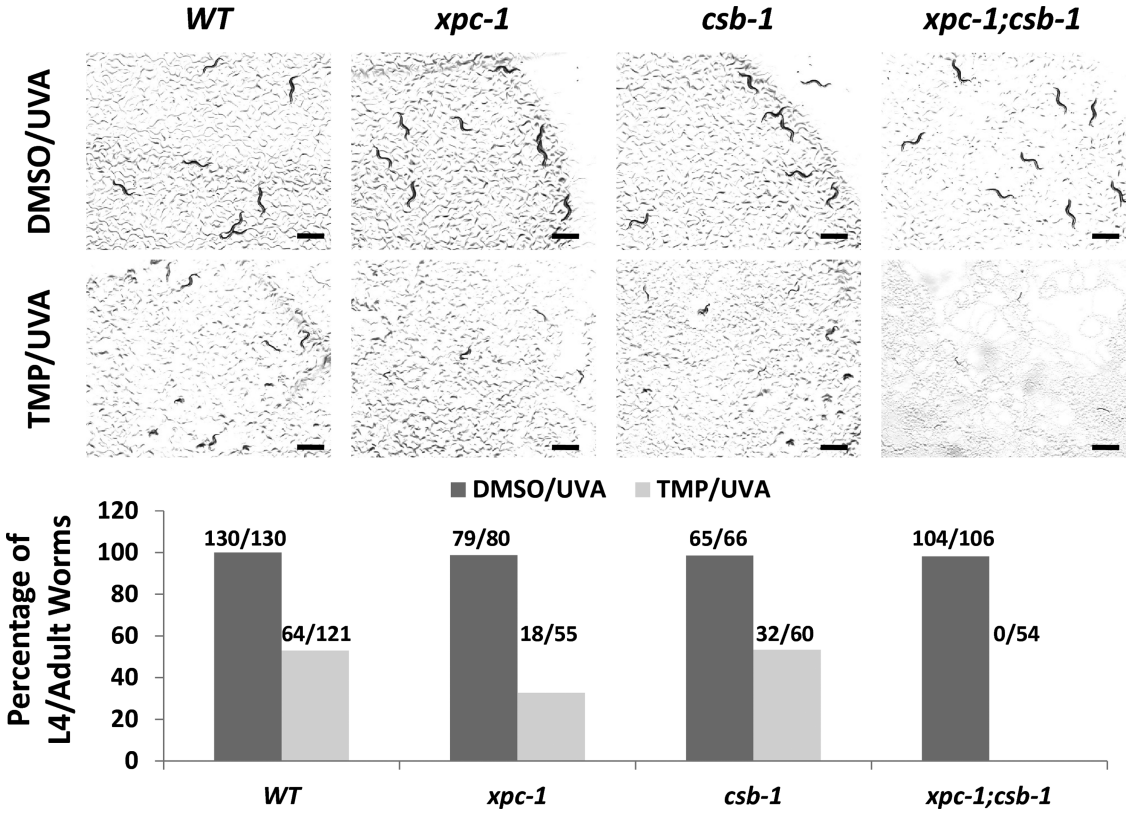

Figure 3. Increased TMP/UVA sensitivity of the *xpc-1;csb-1* double mutant strain in comparison to WT or either single mutant strain alone. (**A**) Visual images. L1 worms were treated with either DMSO or TMP (30 μg/ml) for 60 min, and then UVA irradiated for 60 s. Photographs were taken at day 3 after the designated treatment paradigm. Black bar = 1 mm. (**B**) Sensitivity plots. Plotted is the percentage of L4/adult worms per total for each treatment group from a representative experimental run (number of L4/adult worms per total indicated above).

geal pumping, a phenomenon that (i) engages the pharynx, a neuromuscular tissue that facilitates food intake, (ii) declines as animals age and (iii) is commonly used to assess the functional maintenance of somatic tissue and the health status of the worm. After establishing effective treatment conditions for adult worms, i.e. 30 μg/ml of TMP and 120 s of UVA (TMP/UVA120; ∼960 J/m^2), we determined the relative sensitivities of a select set of mutant animals. Our studies revealed that adult WT worms exhibited a slight, yet statistically insignificant, reduction in pharyngeal pumping behavior at 48 and 72 h post-TMP/UVA120 treatment (Figure 4), whereas a significant defect was seen with the *xpa-1*, *xpf-1*, *ercc-1* and *csb-1*;*xpc-1* mutant strains. Notably, in contrast to what was observed with the L1 animals (see earlier), we found that adult worms deficient only for CSB-1 displayed a robust drop in pharyngeal pumping at 72 h post-treatment, whereas the *xpc-1* mutants did not; the *dog-1* mutant worms appeared like WT as well (Figure 4). These results emphasize a prominent, context-specific role for components of GG-NER and TC-NER in TMP/UVA resistance, and imply that in adults, the latter may take on greater importance due to the post-mitotic nature of the animal.

To determine the contribution of the same set of repair factors in protecting the germline from the adverse effects of DNA ICLs, we treated adult animals with 30 μg/ml of TMP and varying doses of UVA (0, 30, 60 and 120 s), and subsequently measured egg-laying and hatching rates to calculate embryonic survival. We found that embryonic survival in WT animals was increasingly impaired in a UVA dose-dependent manner (Figure 5). Moreover, *xpa-1*, *xpf-1*, *ercc-1, xpc-1*, *csb-1*;*xpc-1* and *dog-1* mutant strains showed a sharp, dose-dependent reduction in the number of viable embryos, with a slightly less pronounced effect seen in *csb-1* animals, at both 3 h and 24 h post-treatment. These results further highlight cell type-specific roles for GG-NER and TC-NER in the response to TMP/UVA-induced genotoxic stress, and reveal that loss of *dog-1*, the ICL-repair factor homolog of FANCJ, uniquely protects the germline from crosslink damage.

Effect of TMP/UVA on longevity

Prior studies have suggested the involvement of naturally occurring DNA ICLs in promoting premature aging features. In particular, a patient harboring a pathogenic *XPF* mutation showed dramatic progeroid symptoms, which were very similar in nature to the phenotypes observed in an ERCC1-defective mouse model and cells isolated from the patient displayed profound crosslinking agent sensitivity in culture (44). To further explore the role that DNA damage might play in the aging process, we determined the lifespan of a set of genetically defined adult worms following a mild TMP/UVA treatment. In brief, WT, *xpf-1*, *xpa-1* and *dog-1* young adult worms were treated with TMP/UVA120,

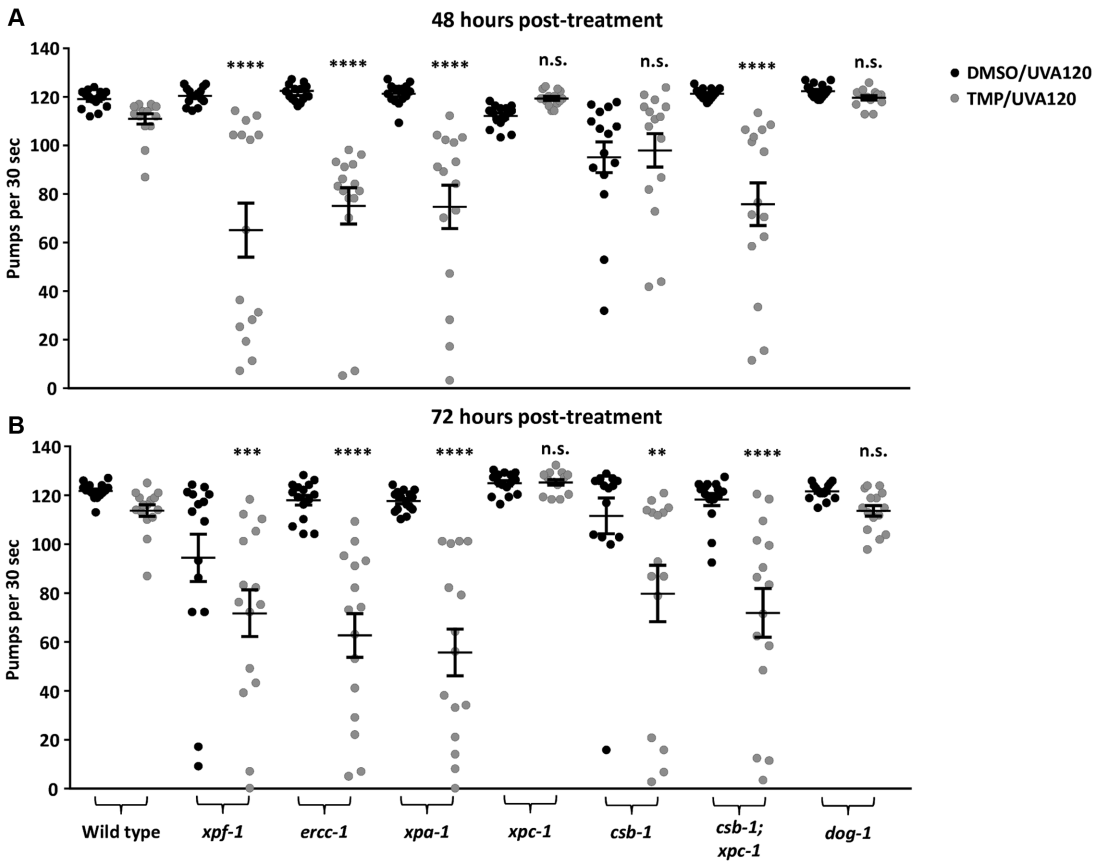

Figure 4. TMP/UVA treatment decreases pumping rates in DNA repair-defective strains. Animals were treated as young adults and pumping rates of individual worms ($n = 15$) were measured for 30 s. (**A**) Pumping rates 48 h after treatment and (**B**) 72 h after treatment of the same population. Significance test was performed in comparison to WT TMP/UVA-treated with $^{**}P < 0.01$, $^{***}P < 0.001$, $^{****}P < 0.0001$ (unpaired, non-parametric Mann–Whitney test). Error bars show SEM.

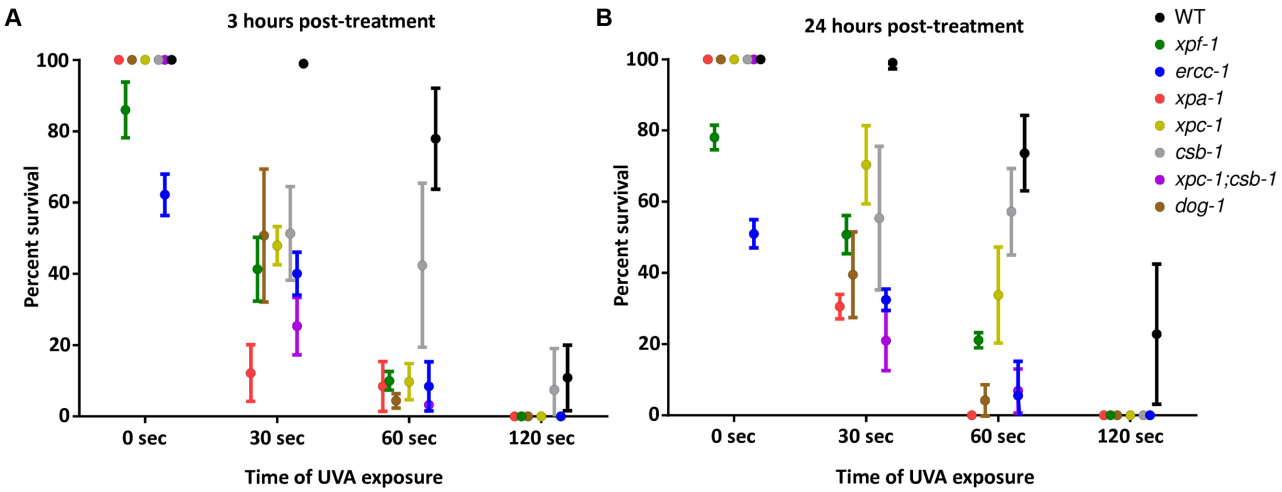

Figure 5. TMP/UVA treatment affects embryonic survival in certain DNA repair-defective strains. Animals were treated as young adults with varying UVA doses and egg laying/hatching rates were measured (**A**) 3 h post-treatment and (**B**) 24 h post-treatment. Error bars show standard deviation.

and then monitored for their structural and physiological fitness. Strikingly, though the *xpf-1* strain did show morphological changes following DMSO/UVA or TMP/UVA treatment at adult day 8 (i.e. reduced size and some tissue decline relative to the unirradiated DMSO control), long-term survival of the mutant worms was not affected by the TMP/UVA120 treatment; a similar overall pattern was observed with the *dog-1* mutant strain, but without the morphological aberrations (Figure 6 and Table 2). Conversely, the combined TMP/UVA120 treatment of the *xpa-1* mutant strain resulted in a significantly reduced lifespan, as well as tissue- and functional-declines that resemble a premature aging phenotype (i.e. reduced mobility, destruction of muscle, intestine and germline tissue, etc.), in comparison to the DMSO and DMSO/UVA controls. These results indicate that genotoxic damage can have profound consequences on the longevity and healthspan of animals in context-specific manners.

DISCUSSION

Using a simple metazoan species (*C. elegans*) and a series of genetically defined mutant animals, we aimed to identify major pathways involved in ICL repair by examining sensitivity to the DNA crosslinking paradigm of TMP plus UVA. Our work specifically determined the effect of TMP/UVA on embryonic survival, larval development, tissue functionality and lifespan in adult animals. Our studies indicate a prominent role for components of the NER pathway, such as XPA and XPF, in resolving toxic DNA crosslink damage. We also uncovered distinct and compensatory roles for the GG-NER and TC-NER sub-pathways in removing ICLs, as revealed by the sensitivity profiles of the *xpc-1*;*csb-1* double mutant strain in comparison to either single mutant alone. Beyond the various NER-related factors, the recombination protein BRC-1 (BRCA1) played a measurable role in TMP/UVA resistance, consistent with HR operating as a prominent pathway in ICL resolution. Conversely, our studies suggest at best a minor role for the MMR system, and no obvious contribution of base excision repair (BER) or non-homologous end-joining (NHEJ), to ICL processing. The role of the FA pathway in ICL removal, at least in somatic cells during larval development, appears to be minor as well (and thus perhaps not well-conserved), since TMP/UVA treatment of the *brc-2* (BRCA2/FANCD1) and *fcd-2* (FANCD2) L1 worms had minimal, if any, effect. Of the three helicases examined, only DOG-1 (FANCJ/BRIP1/BACH1), and not the WRN or BLM homologs, was found to participate in the clearance of toxic crosslinks from the genome of developing animals; DOG-1 also functioned in protecting the germline, but not somatic tissues, such as the pharynx, when TMP/UVA was administered at the young adult stage. Of the nucleases outside of classic NER, only MUS-81 and to a lesser extent EXO-1, showed clear roles in coping up with the TMP/UVA-induced DNA damage in the whole organism. Loss of *fan-1* or *slx-1* resulted in germline-restricted sensitivity, revealing context-dependent contributions of these two nucleases in our experimental paradigm; no obvious role was observed for the GEN-1 or MRT-1 (SNM1) nucleases in DNA ICL repair.

Our studies involving the treatment of L1 worms indicate prominent roles for the *C. elegans* homologs of XPF, ERCC1, XPA and XPG in the protection against the devastating effects of DNA ICLs. A function for the XPF-ERCC1 structure-specific endonuclease in ICL repair has long been recognized, where the enzyme complex is presumably responsible for cleaving 5′ to the crosslink to initiate the unhooking process (45). Defects in this protein complex have been associated with profound cellular sensitivity to DNA crosslinking agents, as well as the genetic disorders xeroderma pigmentosum, XFE progeria syndrome, FA and CS, which are characterized by developmental shortcomings, cancer predisposition and/or premature aging features (16). Although under-appreciated and often incorrectly presented in the literature (discussed in (19)), there are multiple lines of evidence indicating roles for other NER factors, e.g. XPA, XPB, XPD and XPG, in ICL repair. XPA is a non-enzymatic DNA binding protein that participates in both GG-NER and TC-NER, enabling damage-verification and assembly of the NER incision complexes after recognition by either XPC or the TC-NER (CSB) machinery; XPA has also been shown to directly interact with the XPF-ERCC1 nuclease (46). XPG, a separate structure-specific endonuclease in classic NER, has been suggested to enable the initial unhooking process by cleaving 3′ to the ICL, at least in one repair scenario (47). While the prominence of the NER pathways in ICL resistance appears to be maintained in lower eukaryotes, namely the budding yeast *Saccharomyces cerevisiae* (48), the NER systems have seemingly reorganized their overall contributions in humans, with perhaps a movement toward the more complex FA/HR-associated processes, particularly in actively dividing cells (discussed further below). Nevertheless, the sensitivity findings presented here strongly support the existence of replication/recombination-independent mechanisms that engage core NER factors to carry out recognition and excision of DNA ICLs (26,49) (Figure 7, left).

Treatment of either L1 or young adult worms with TMP/UVA provided a distinct picture of the relative contributions of the NER proteins/pathways to ICL repair. In *C. elegans*, most somatic cell divisions occur during early embryogenesis, when 558 of the total 959 somatic cells are born. In the ensuing larval development phase (L1–L4; Supplementary Figure S1), the differentiated cells grow mostly in size, with limited overall cell division. In adult animals, the somatic tissues are entirely terminally differentiated (i.e. non-replicating and post-mitotic), with only germ cells participating in active proliferation. These features of the nematode's biology allow assessment of the distinct involvement of DNA repair pathways in proliferating embryonic or germ cells or mostly post-mitotic somatic cells. In our analysis, the *xpf-1*, *ercc-1*, *xpa-1* and *csb-1;xpc-1* mutant strains were found to exhibit robust hypersensitivity to TMP/UVA independent of the treatment stage, while the protective role of XPC and CSB was dependent on the timing of genotoxin administration. Specifically, the *xpc-1* mutant strain was only hypersensitive (in comparison to WT worms) when treated at the L1 stage, and not in early adulthood, whereas the *csb-1* mutant strain showed the reverse phenotype. Thus, our data indicate that GG-NER is a major repair route for ICL removal during de-

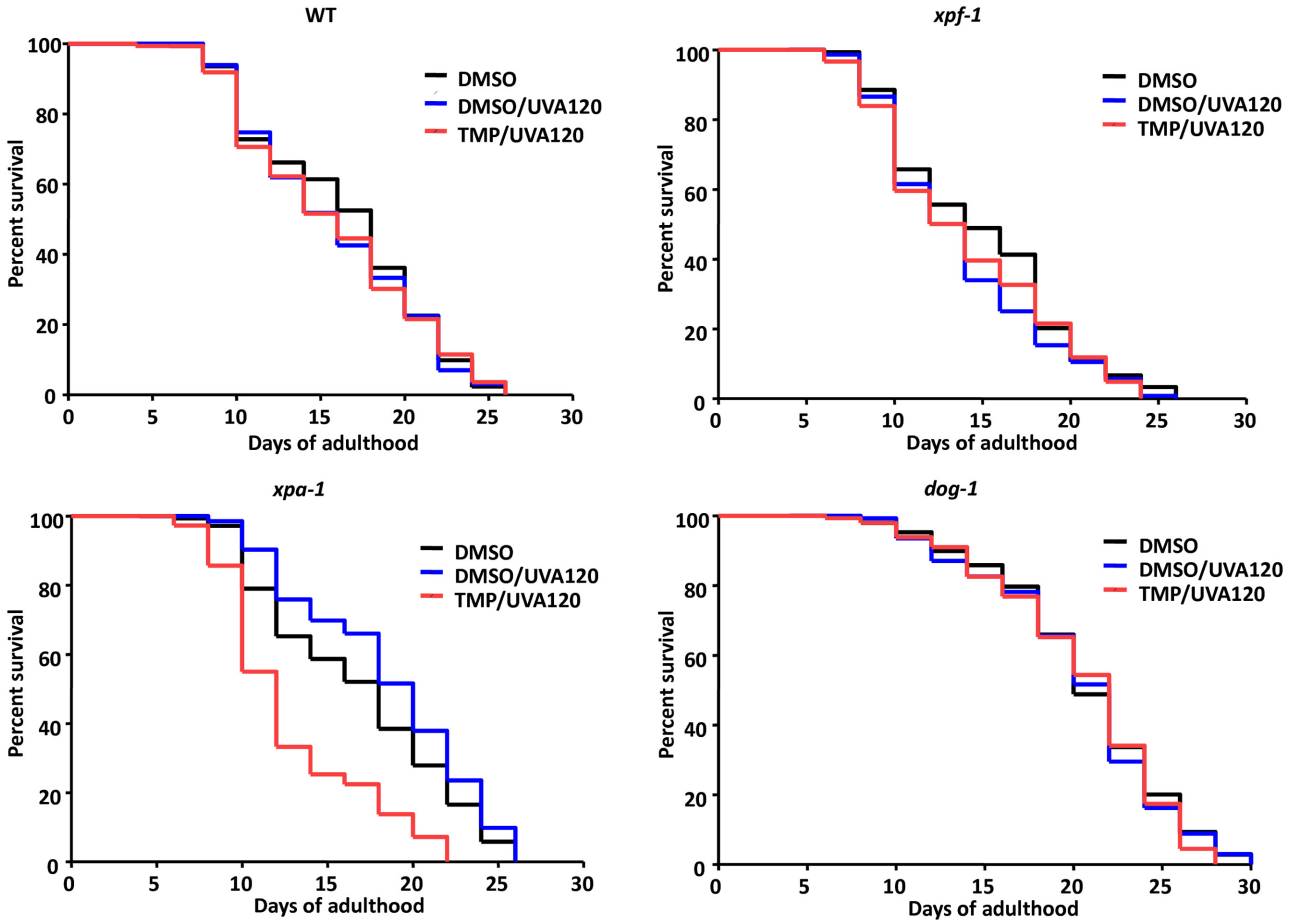

Figure 6. Effect of TMP/UVA treatment on lifespan of select DNA repair-defective strains. Animals were treated as young adults (day 0) with either DMSO-only (black), DMSO/UVA (2 min; blue), or DMSO/UVA (2 min) and TMP (black), and lifespan was measured until death of the population (compare Table 2).

Table 2. Consequences of TMP/UVA genomic damage on lifespan

Genotype	Death events	Censored events	Median lifespan	Max. lifespan	*P*-value
WT (DMSO)	147/97	14/14	18.0 ± 0.0	26.0 ± 0.0	
WT (DMSO/UVA)	134/97	14/22	17.0 ± 1.0	26.0 ± 0.0	$P > 0.5$
WT (TMP/UVA)	142/108	3/12	16.0 ± 0.0	26.0 ± 0.0	$P > 0.5$
xpf-1 (DMSO)	120/129	32/23	14.0 ± 0.0	26.0 ± 0.0	
xpf-1 (DMSO/UVA)	130/136	26/20	13.0 ± 1.0	25.0 ± 1.0	$P > 0.5$
xpf-1 (TMP/UVA)	146/149	5/2	13.0 ± 1.0	25.0 ± 1.0	$P > 0.5$
xpa-1 (DMSO)	133/103	18/14	18.0 ± 0.0	26.0 ± 0.0	
xpa-1 (DMSO/UVA)	132/84	11/39	20.0 ± 0.0	26.5 ± 0.5	$P < 0.001$
xpa-1 (TMP/UVA)	140/142	10/8	12.0 ± 0.0	22.0 ± 0.0	$P < 0.0001$
dog-1 (DMSO)	144/108	12/12	20.0 ± 0.0	30.0 ± 0.0	
dog-1 (DMSO/UVA)	136/90	8/8	22.0 ± 0.0	29.0 ± 1.0	$P > 0.5$
dog-1 (TMP/UVA)	137/94	15/14	22.0 ± 0.0	30.0 ± 0.0	$P > 0.5$

Shown are the raw results of two independent lifespan experiments (separated by a dash). Young adult worms of the indicated genotype were treated as designated and monitored for survival. Both death and censored events are reported, as are the median and maximal lifespan. The *P*-values are calculated based on comparison of DMSO/UVA120 or TMP/UVA120 to the DMSO-only control using Kaplan–Meier survival analysis.

velopment. TC-NER becomes more critical for resolution of ICLs when the animal is fully developed and all cells are terminally-differentiated. This picture is broadly consistent with the egg-laying and hatching experiments, where GG-NER was found to have a more significant role in protecting the germline from crosslink damage. Notably, the role of GG-NER in the removal of UV-induced cyclobutane-pyrimidine dimers and 6–4 photoproducts is more restricted to the rapid cell division cycles during early embryogenesis and in proliferating germ cells, while somatic tissues rely mostly on TC-NER during early larval development (50,51).

Another notable observation is that only the *xpa-1* mutant strain, and not the *xpf-1* or *dog-1* mutant strains,

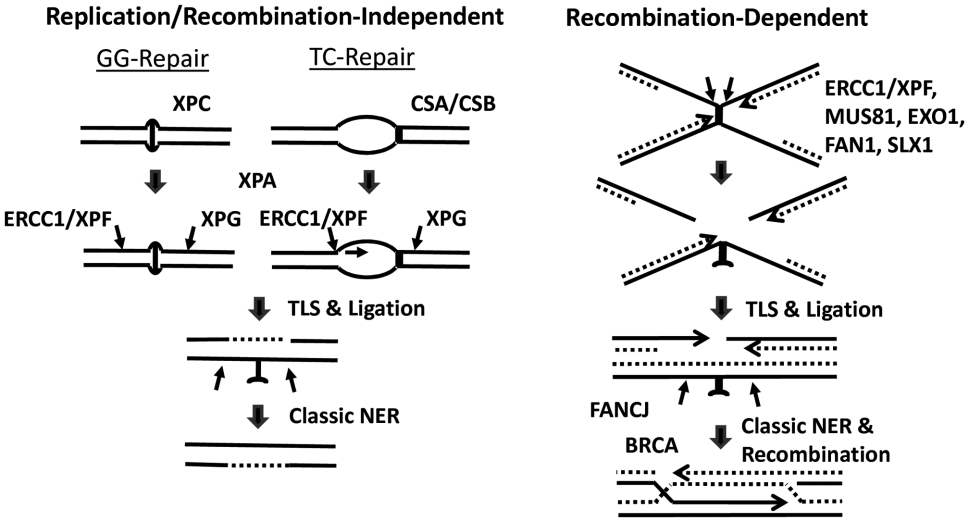

Figure 7. Replication-independent and -dependent mechanisms of ICL repair. (Left) Global genome (GG) and transcription-coupled (TC) repair responses. GG-repair is initiated upon XPC damage recognition. TC-repair is called into action upon RNA polymerase II stalling at a transcription blocking lesion, followed by assembly of the repair machinery that involves proteins such as CSA and CSB. From this point, both pathways proceed, in all likelihood, via the same mechanism, which includes incisions to unhook the crosslink by ERCC1/XPF and XPG; or via 5′ to 3′ exonuclease degradation across the ICL. Following translesion synthesis (TLS) across the crosslink remnant and nick ligation, a round of classic NER is thought to be conducted to restore the genome back to its original state. (Right) Recombination-mediated ICL resolution. Upon replication fork collision with a DNA ICL, and independent of traverse, dual incisions are carried out by nucleases (listed) in a substrate-specific or cell type-specific manner to unhook the crosslink. Following TLS and ligation, classic NER generates an undamaged and intact chromosome duplex, which is used as the homologous template to carry-out classic recombination repair involving BRCA1 and RAD51. Helicases, namely DOG-1 (FANCJ), also appear to be involved at some point in the process.

showed a shortened lifespan following TMP/UVA treatment when challenged as a young adult. Though the *dog-1* observation likely stems from its primary role being in replication-associated ICL repair, the lack of an effect of TMP/UVA on *xpf-1* longevity is more difficult to explain. One possibility is that *xpf-1* mutant animals, which already exhibit a shortened life expectancy in comparison to WT, are minimally impacted (in terms of longevity, but not pumping) by the additional burden of ICLs introduced by TMP/UVA treatment. Alternatively, there may exist other mechanisms to carry out unhooking in post-mitotic cells that don't require the 5′ incision event of the XPF/ERCC1 nuclease complex, something that can be evaluated through epistasis analysis. The finding that *xpa-1* mutant animals display a wide range of pathologies and a reduced life expectancy following TMP/UVA treatment highlights that (i) this general NER factor plays a critical role in crosslink repair in all cell types and (ii) persistent DNA damage severely disturbs tissue homeostasis and imparts a prematurely-aged physical appearance in *C. elegans* (52).

Recombination pathways, namely HR, have been well documented for their involvement in resolving DNA structures that are formed upon replication fork collapse at a DNA ICL (53). Our data certainly point to HR, and not NHEJ, in contributing to TMP/UVA resistance, as gleaned from the sensitivity profiles of the *brc-1* (increased) and *cku-80* (no effect) mutant strains, respectively. The somewhat mild hypersensitivity of the *brc-1* mutant may indicate that RAD51-mediated HR is still operational, although functioning at reduced efficiency, in the absence of the BRCA1 protein. Alternatively, due to their intrinsic biology as discussed above, worms may rely more on the NER-directed pathways for ICL resolution than the recombination-dependent mechanisms (Figure 7). Indeed, such a feature would indicate that worms employ ICL removal strategies more in-line with those favored by bacteria and yeast (48). Going forward, it will be worthwhile to more extensively investigate how distinct mammalian tissues, particularly post-mitotic cell types, utilize NER for ICL repair.

The contribution of the FA pathway to ICL resolution appears to be complex in *C. elegans*. Mutations in the *BRCA* genes in humans have been linked to breast and ovarian cancer predisposition, as well as to FA, a genetic disorder diagnosed by crosslinking agent hypersensitivity (54). While our studies uncovered an important role for BRC-1 (BRCA1) in TMP/UVA resistance, we did not see a similar contribution for the related factors, BRC-2 (BRCA2/FANCD1) or FCD-2 (FANCD2). Our work furthermore supports a role for the DOG-1 helicase, which is homologous to FANCJ/BRIP1/BACH1 in humans, in the ICL response, an observation that is consistent with a prior study (36). As mentioned above, the finding that the *dog-1* mutant strain exhibits measurable sensitivity to TMP/UVA when treated at the L1 stage, or as a young adult, but only in the germline, is consistent with a selective role for the protein in the replication-associated responses (Figure 7, right). Thus, in total, our studies suggest that BRC-1 and DOG-1 possess functions outside of the classic FA response and/or that the FA pathway plays a quantitatively lesser role relative to the NER-related mechanisms in ICL resolution in worms. It will therefore be interesting in the future to expand our germline sensitivity analysis to include all FA components, as its seems reasonable to predict that the major functions for the FA/HR-associated processes in ICL repair will be most prominent in cycling cells where replication-dependent events predominant. De-

spite the studies that indicate a role in ICL resolution for the WRN and BLM helicases, which are defective in the genetic disorders Werner and Bloom, respectively, we observed no detectable contribution of the homologs in worms (note: WRN-1 lacks the exonuclease domain found in the human protein) to TMP/UVA resistance, implying that their intrinsic activities are irrelevant to the major eukaryotic ICL responses or have evolved to be more specialized, possibly in some back-up capacity, in mammalian ICL repair (55).

Besides the nucleases involved in NER (see above), we examined (using the L1 treatment strategy) the protective role of a range of other conserved processing enzymes, some of which have been reported to be involved in ICL repair (56). We did not observe any obvious role for the Holliday-junction endonuclease, GEN-1, in TMP/UVA resistance, consistent with the major function of this enzyme being in the resolution of HR DNA crossover intermediates that arise because of failed replication events (57). We also did not see a clear contribution of MRT-1 in protecting against TMP/UVA genotoxicity, a finding that seemingly conflicts with prior reports describing a function for the SNM1 proteins in ICL repair (33,58,59). This apparent discrepancy may stem from the fact that mammals harbor three SNM1 (PSO2) paralogs (SNM1A, SNM1B/Apollo and Artemis), each potentially having acquired a specialized function in DNA metabolism, such as SNM1A in ICL repair. MUS-81, a structure-specific endonuclease, was found to play a clear and reproducible role in TMP/UVA resistance, though not to the same extent as XPF-ERCC1. This observation is ostensibly in-line with prior work suggesting that the MUS81-EME1 nuclease complex acts only on a subset of DNA intermediates generated after a replication fork collides with an ICL (56). Our results are some of the first to implicate a function for EXO-1 in DNA ICL repair (60), albeit a relatively minor one. As a 5′-3′ exonuclease and 5′-flap endonuclease (61), the enzyme may operate in a manner similar to MUS81, in that EXO1 may participate in the resolution of a particular subset of DNA structures formed during the ICL repair response. Finally, our studies indicate a critical role for the structure-specific nucleases FAN-1 and SLX-1 in specifically protecting the meiotic germline, whereas no obvious defects were seen in the mitotic tissue of the corresponding mutant worms in comparison to WT. This finding implies non-redundant, essential roles for these two nucleases in specific replication-dependent ICL repair events, perhaps explaining some of the apparent anomalies regarding the molecular participation of FAN1 and SLX1 in ICL resolution and the varying clinical phenotypes associated with genetic defects in the different nuclease factors (56).

The contribution of MMR to ICL repair is presently uncertain (29,62). In particular, published work has indicated recognition of ICLs by the initiating complexes of MMR (e.g. MSH2-MSH3), yet defects in the core MMR proteins have been found to inconsistently affect cellular sensitivity to agents that induce ICLs, and often lead to increased resistance. Our studies reveal a subtle, albeit reproducible, adverse effect of MSH-2 deficiency on TMP/UVA sensitivity. This sensitivity appeared primarily as reduced egg laying, a phenotype that could result from either a mitotic (reduced egg release) or meiotic (reduced egg production or hatching) defect. In addition, there is emerging evidence suggesting that BER may affect ICL processing events (63). However, our results do not support BER playing a major role in protecting against TMP/UVA-induced ICLs. Nevertheless, it is important to emphasize that the BER system present in *C. elegans* is quite distinct from mammals, in that it lacks classic BER proteins such as the 8-oxoguanine DNA glycosylase (OGG1), the endonuclease eight (NEIL) homologs, the scaffold protein X-ray cross-complementing 1 (XRCC1) and a DNA polymerase β homolog; thus, the participation of the BER process in ICL responses would seemingly be best characterized in mammalian model systems.

In closing, the work presented herein has established a platform to use *C. elegans* as a model system to define pathways relevant to DNA crosslink repair during development and aging, particularly their roles in mitotically and meiotically proliferating and terminally differentiated cell and tissue types. Our studies have revealed prominent roles for the two sub-pathways of NER, i.e. GG-NER and TC-NER, with their relative contributions depending on the time of ICL induction (e.g. during development or adulthood). We have also corroborated a significant role for HR (BRC-1/BRCA1) in ICL repair, yet observed little or no role for MMR, NHEJ and BER in TMP/UVA resistance. Our findings documented a distinct response for the various FA-related components to crosslink induction, suggestive of a possible organism- or cell type-specific function for the FA pathway in ICL resolution. Last, we uncovered significant, albeit restricted, contributions of the DOG-1/FANCJ helicase and the MUS-81, EXO-1, FAN-1 and SLX-1 nucleases, but no obvious role for the *C. elegans* homologs of BRCA2/FANCD1, WRN, BLM, SNM1 and GEN1, in ICL processing. Going forward, this system will permit more exhaustive analysis into the contribution of other proteins to ICL repair, as well as the epistatic nature of the repair components and mechanisms uncovered.

SUPPLEMENTARY DATA

Supplementary Data are available at NAR Online.

ACKNOWLEDGEMENTS

We thank Drs Robert Brosh and Marina Bellani at the National Institutes on Aging for critical reading of the manuscript. Worm strains were provided by the National Bioresource Project and the Caenorhabditis Genetics Center.

FUNDING

Deutsche Forschungsgemeinschaft [CECAD, SFB 829, SFB 670, KFO 286]; European Commission (ERC Starting Grant) [260383, FP7-PEOPLE-2012-ITN CodeAge 316354, aDDRess 316390, MARRIAGE 316964, Flag-Era-JTC2015 GRAPHENE]; Bundesministerium für Bildung und Forschung [Sybacol FKZ0315893A-B]; COST Action [BM1408, GENiE] (BS); National Institute on Aging, Intramural Research Program, NIH [AG000751] (DMWIII). Funding for open access charge: National Institute on Aging, Intramural Research Program, NIH.
Conflict of interest statement. None declared.

REFERENCES

1. Lindahl,T. (1993) Instability and decay of the primary structure of DNA. *Nature*, **362**, 709–715.
2. Cadet,J., Ravanat,J.L., TavernaPorro,M., Menoni,H. and Angelov,D. (2012) Oxidatively generated complex DNA damage: tandem and clustered lesions. *Cancer Lett.*, **327**, 5–15.
3. Ribezzo,F., Shiloh,Y. and Schumacher,B. (2016) Systemic DNA damage responses in aging and diseases. *Semin. Cancer Biol.*, **37–38**, 26–35.
4. Muniandy,P.A., Liu,J., Majumdar,A., Liu,S.T. and Seidman,M.M. (2010) DNA interstrand crosslink repair in mammalian cells: step by step. *Crit. Rev. Biochem. Mol. Biol.*, **45**, 23–49.
5. Niedernhofer,L.J., Daniels,J.S., Rouzer,C.A., Greene,R.E. and Marnett,L.J. (2003) Malondialdehyde, a product of lipid peroxidation, is mutagenic in human cells. *J. Biol. Chem.*, **278**, 31426–31433.
6. Johnson,K.M., Price,N.E., Wang,J., Fekry,M.I., Dutta,S., Seiner,D.R., Wang,Y. and Gates,K.S. (2013) On the formation and properties of interstrand DNA-DNA cross-links forged by reaction of an abasic site with the opposing guanine residue of 5′-CAp sequences in duplex DNA. *J. Am. Chem. Soc.*, **135**, 1015–1025.
7. Price,N.E., Johnson,K.M., Wang,J., Fekry,M.I., Wang,Y. and Gates,K.S. (2014) Interstrand DNA-DNA cross-link formation between adenine residues and abasic sites in duplex DNA. *J. Am. Chem. Soc.*, **136**, 3483–3490.
8. Deans,A.J. and West,S.C. (2011) DNA interstrand crosslink repair and cancer. *Nat. Rev. Cancer*, **11**, 467–480.
9. Hashimoto,S., Anai,H. and Hanada,K. (2016) Mechanisms of interstrand DNA crosslink repair and human disorders. *Genes Environ.*, **38**, 9.
10. Walden,H. and Deans,A.J. (2014) The Fanconi anemia DNA repair pathway: structural and functional insights into a complex disorder. *Annu. Rev. Biophys.*, **43**, 257–278.
11. Jones,M.J. and Huang,T.T. (2012) The Fanconi anemia pathway in replication stress and DNA crosslink repair. *Cell Mol. Life Sci.*, **69**, 3963–3974.
12. Constantinou,A. (2012) Rescue of replication failure by Fanconi anaemia proteins. *Chromosoma*, **121**, 21–36.
13. Crossan,G.P. and Patel,K.J. (2012) The Fanconi anaemia pathway orchestrates incisions at sites of crosslinked DNA. *J. Pathol.*, **226**, 326–337.
14. Klein,D.D., Boonen,R.A., Long,D.T., Szypowska,A.A., Raschle,M., Walter,J.C. and Knipscheer,P. (2014) XPF-ERCC1 acts in Unhooking DNA interstrand crosslinks in cooperation with FANCD2 and FANCP/SLX4. *Mol. Cell*, **54**, 460–471.
15. Hodskinson,M.R., Silhan,J., Crossan,G.P., Garaycoechea,J.I., Mukherjee,S., Johnson,C.M., Scharer,O.D. and Patel,K.J. (2014) Mouse SLX4 is a tumor suppressor that stimulates the activity of the nuclease XPF-ERCC1 in DNA crosslink repair. *Mol. Cell*, **54**, 472–484.
16. Manandhar,M., Boulware,K.S. and Wood,R.D. (2015) The ERCC1 and ERCC4 (XPF) genes and gene products. *Gene*, **569**, 153–161.
17. Roy,U. and Scharer,O.D. (2016) Involvement of translesion synthesis DNA polymerases in DNA interstrand crosslink repair. *DNA Repair (Amst)*, **44**, 33–41.
18. Huang,J., Liu,S., Bellani,M.A., Thazhathveetil,A.K., Ling,C., de Winter,J.P., Wang,Y., Wang,W. and Seidman,M.M. (2013) The DNA translocase FANCM/MHF promotes replication traverse of DNA interstrand crosslinks. *Mol. Cell*, **52**, 434–446.
19. Wood,R.D. (2010) Mammalian nucleotide excision repair proteins and interstrand crosslink repair. *Environ. Mol. Mutagen.*, **51**, 520–526.
20. Wang,A.T., Sengerova,B., Cattell,E., Inagawa,T., Hartley,J.M., Kiakos,K., Burgess-Brown,N.A., Swift,L.P., Enzlin,J.H., Schofield,C.J. *et al.* (2011) Human SNM1A and XPF-ERCC1 collaborate to initiate DNA interstrand cross-link repair. *Genes Dev.*, **25**, 1859–1870.
21. Spivak,G. (2016) Transcription-coupled repair: an update. *Arch. Toxicol.*, **90**, 2583–2594.
22. Zhang,N., Lu,X., Zhang,X., Peterson,C.A. and Legerski,R.J. (2002) hMutSbeta is required for the recognition and uncoupling of psoralen interstrand cross-links in vitro. *Mol. Cell. Biol.*, **22**, 2388–2397.
23. Zhao,J., Jain,A., Iyer,R.R., Modrich,P.L. and Vasquez,K.M. (2009) Mismatch repair and nucleotide excision repair proteins cooperate in the recognition of DNA interstrand crosslinks. *Nucleic Acids Res.*, **37**, 4420–4429.
24. Zhu,G. and Lippard,S.J. (2009) Photoaffinity labeling reveals nuclear proteins that uniquely recognize cisplatin-DNA interstrand cross-links. *Biochemistry*, **48**, 4916–4925.
25. Wu,Q., Christensen,L.A., Legerski,R.J. and Vasquez,K.M. (2005) Mismatch repair participates in error-free processing of DNA interstrand crosslinks in human cells. *EMBO Rep.*, **6**, 551–557.
26. Enoiu,M., Jiricny,J. and Scharer,O.D. (2012) Repair of cisplatin-induced DNA interstrand crosslinks by a replication-independent pathway involving transcription-coupled repair and translesion synthesis. *Nucleic Acids Res.*, **40**, 8953–8964.
27. Zhu,G., Song,L. and Lippard,S.J. (2013) Visualizing inhibition of nucleosome mobility and transcription by cisplatin-DNA interstrand crosslinks in live mammalian cells. *Cancer Res.*, **73**, 4451–4460.
28. Papouli,E., Cejka,P. and Jiricny,J. (2004) Dependence of the cytotoxicity of DNA-damaging agents on the mismatch repair status of human cells. *Cancer Res.*, **64**, 3391–3394.
29. Vasquez,K.M. (2010) Targeting and processing of site-specific DNA interstrand crosslinks. *Environ. Mol. Mutagen.*, **51**, 527–539.
30. Moor,A.C. and Gasparro,F.P. (1996) Biochemical aspects of psoralen photochemotherapy. *Clin. Dermatol.*, **14**, 353–365.
31. Rose,A. (2014) Replication and repair. *WormBook*, 1–16.
32. Lans,H. and Vermeulen,W. (2015) Tissue specific response to DNA damage: C. elegans as role model. *DNA Repair (Amst)*, **32**, 141–148.
33. Meier,B., Barber,L.J., Liu,Y., Shtessel,L., Boulton,S.J., Gartner,A. and Ahmed,S. (2009) The MRT-1 nuclease is required for DNA crosslink repair and telomerase activity in vivo in Caenorhabditis elegans. *EMBO J.*, **28**, 3549–3563.
34. Smogorzewska,A., Desetty,R., Saito,T.T., Schlabach,M., Lach,F.P., Sowa,M.E., Clark,A.B., Kunkel,T.A., Harper,J.W., Colaiacovo,M.P. *et al.* (2010) A genetic screen identifies FAN1, a Fanconi anemia-associated nuclease necessary for DNA interstrand crosslink repair. *Mol. Cell*, **39**, 36–47.
35. Collis,S.J., Barber,L.J., Ward,J.D., Martin,J.S. and Boulton,S.J. (2006) C. elegans FANCD2 responds to replication stress and functions in interstrand cross-link repair. *DNA Repair (Amst)*, **5**, 1398–1406.
36. Youds,J.L., Barber,L.J., Ward,J.D., Collis,S.J., O'Neil,N.J., Boulton,S.J. and Rose,A.M. (2008) DOG-1 is the Caenorhabditis elegans BRIP1/FANCJ homologue and functions in interstrand cross-link repair. *Mol. Cell. Biol.*, **28**, 1470–1479.
37. Lee,K.Y., Chung,K.Y. and Koo,H.S. (2010) The involvement of FANCM, FANCI, and checkpoint proteins in the interstrand DNA crosslink repair pathway is conserved in C. elegans. *DNA Repair (Amst)*, **9**, 374–382.
38. Brenner,S. (1974) The genetics of Caenorhabditis elegans. *Genetics*, **77**, 71–94.
39. Porta-de-la-Riva,M., Fontrodona,L., Villanueva,A. and Ceron,J. (2012) Basic Caenorhabditis elegans methods: synchronization and observation. *J. Vis. Exp.*, e4019.
40. Yandell,M.D., Edgar,L.G. and Wood,W.B. (1994) Trimethylpsoralen induces small deletion mutations in Caenorhabditis elegans. *Proc. Natl. Acad. Sci. U.S.A.*, **91**, 1381–1385.
41. Saito,T.T., Youds,J.L., Boulton,S.J. and Colaiacovo,M.P. (2009) Caenorhabditis elegans HIM-18/SLX-4 interacts with SLX-1 and XPF-1 and maintains genomic integrity in the germline by processing recombination intermediates. *PLoS. Genet.*, **5**, e1000735.
42. Iyama,T., Lee,S.Y., Berquist,B.R., Gileadi,O., Bohr,V.A., Seidman,M.M., McHugh,P.J. and Wilson,D.M. III (2015) CSB interacts with SNM1A and promotes DNA interstrand crosslink processing. *Nucleic Acids Res.*, **43**, 247–258.
43. Alekseev,S. and Coin,F. (2015) Orchestral maneuvers at the damaged sites in nucleotide excision repair. *Cell Mol. Life Sci.*, **72**, 2177–2186.
44. Niedernhofer,L.J., Garinis,G.A., Raams,A., Lalai,A.S., Robinson,A.R., Appeldoorn,E., Odijk,H., Oostendorp,R., Ahmad,A., van,L.W. *et al.* (2006) A new progeroid syndrome reveals that genotoxic stress suppresses the somatotroph axis. *Nature*, **444**, 1038–1043.
45. Kuraoka,I., Kobertz,W.R., Ariza,R.R., Biggerstaff,M., Essigmann,J.M. and Wood,R.D. (2000) Repair of an interstrand DNA cross-link initiated by ERCC1-XPF repair/recombination nuclease. *J. Biol. Chem.*, **275**, 26632–26636.

46. Sugitani,N., Sivley,R.M., Perry,K.E., Capra,J.A. and Chazin,W.J. (2016) XPA: A key scaffold for human nucleotide excision repair. *DNA Repair (Amst)*, **44**, 123–135.
47. Evans,E., Fellows,J., Coffer,A. and Wood,R.D. (1997) Open complex formation around a lesion during nucleotide excision repair provides a structure for cleavage by human XPG protein. *EMBO J.*, **16**, 625–638.
48. McVey,M. (2010) Strategies for DNA interstrand crosslink repair: insights from worms, flies, frogs, and slime molds. *Environ. Mol. Mutagen.*, **51**, 646–658.
49. Wang,X., Peterson,C.A., Zheng,H., Nairn,R.S., Legerski,R.J. and Li,L. (2001) Involvement of nucleotide excision repair in a recombination-independent and error-prone pathway of DNA interstrand cross-link repair. *Mol. Cell. Biol.*, **21**, 713–720.
50. Lans,H., Marteijn,J.A., Schumacher,B., Hoeijmakers,J.H., Jansen,G. and Vermeulen,W. (2010) Involvement of global genome repair, transcription coupled repair, and chromatin remodeling in UV DNA damage response changes during development. *PLoS. Genet.*, **6**, e1000941.
51. Mueller,M.M., Castells-Roca,L., Babu,V., Ermolaeva,M.A., Muller,R.U., Frommolt,P., Williams,A.B., Greiss,S., Schneider,J.I., Benzing,T. *et al.* (2014) DAF-16/FOXO and EGL-27/GATA promote developmental growth in response to persistent somatic DNA damage. *Nat. Cell. Biol.*, **16**, 1168–1179.
52. Lans,H., Lindvall,J.M., Thijssen,K., Karambelas,A.E., Cupac,D., Fensgard,O., Jansen,G., Hoeijmakers,J.H., Nilsen,H. and Vermeulen,W. (2013) DNA damage leads to progressive replicative decline but extends the life span of long-lived mutant animals. *Cell Death Differ.*, **20**, 1709–1718.
53. Hinz,J.M. (2010) Role of homologous recombination in DNA interstrand crosslink repair. *Environ. Mol. Mutagen.*, **51**, 582–603.
54. Michl,J., Zimmer,J. and Tarsounas,M. (2016) Interplay between Fanconi anemia and homologous recombination pathways in genome integrity. *EMBO J.*, **35**, 909–923.
55. Suhasini,A.N. and Brosh,R.M. Jr (2012) Fanconi anemia and Bloom's syndrome crosstalk through FANCJ-BLM helicase interaction. *Trends Genet.*, **28**, 7–13.
56. Zhang,J. and Walter,J.C. (2014) Mechanism and regulation of incisions during DNA interstrand cross-link repair. *DNA Repair (Amst)*, **19**, 135–142.
57. Sarbajna,S. and West,S.C. (2014) Holliday junction processing enzymes as guardians of genome stability. *Trends Biochem. Sci.*, **39**, 409–419.
58. Cattell,E., Sengerova,B. and McHugh,P.J. (2010) The SNM1/Pso2 family of ICL repair nucleases: from yeast to man. *Environ. Mol. Mutagen.*, **51**, 635–645.
59. Yan,Y., Akhter,S., Zhang,X. and Legerski,R. (2010) The multifunctional SNM1 gene family: not just nucleases. *Future Oncol.*, **6**, 1015–1029.
60. Ward,T.A., Dudasova,Z., Sarkar,S., Bhide,M.R., Vlasakova,D., Chovanec,M. and McHugh,P.J. (2012) Components of a Fanconi-like pathway control Pso2-independent DNA interstrand crosslink repair in yeast. *PLoS Genet.*, **8**, e1002884.
61. Lee,B.I. and Wilson,D.M. III (1999) The RAD2 domain of human exonuclease 1 exhibits 5′ to 3′ exonuclease and flap structure-specific endonuclease activities. *J. Biol. Chem.*, **274**, 37763–37769.
62. Cantor,S.B. and Brosh,R.M. Jr (2014) What is wrong with Fanconi anemia cells? *Cell Cycle*, **13**, 3823–3827.
63. Kothandapani,A. and Patrick,S.M. (2013) Evidence for base excision repair processing of DNA interstrand crosslinks. *Mutat. Res.*, **743–744**, 44–52.